

Mitochondrial Responses to Sublethal Doxorubicin in H9c2 Cardiomyocytes: The Role of Phosphorylated CaMKII

Agung Kurniawan Priyono,* Junichiro Miake,* Tatsuya Sawano,* Yoshinori Ichihara,* Keiko Nagata,* Akihiro Okamura,† Takuya Tomomori,† Aiko Takami,† Tomomi Notsu,‡ Kazuhiro Yamamoto† and Takeshi Imamura*

*Division of Pharmacology, Department of Pathophysiological and Therapeutic Sciences, School of Medicine, Faculty of Medicine, Tottori University, Yonago 683-8503, Japan, †Division of Cardiovascular Medicine and Endocrinology and Metabolism, Department of Multidisciplinary Internal Medicine, School of Medicine, Faculty of Medicine, Tottori University, Yonago 683-8504, Japan, and ‡Division of Regenerative Medicine and Therapeutics, Department of Genomic Medicine and Regenerative Therapy, School of Medicine, Faculty of Medicine, Tottori University, Yonago 683-8503, Japan

ABSTRACT

Background Doxorubicin (Dox) is effective against different types of cancers, but it poses cardiotoxic side effects, frequently resulting in irreversible heart failure. However, the complexities surrounding this cardiotoxicity, especially at sublethal dosages, remain to be fully elucidated. We investigated early cellular disruptions in response to sublethal Dox, with a specific emphasis on the role of phosphorylated calcium/calmodulin-dependent protein kinase II (CaMKII) in initiating mitochondrial dysfunction.

Methods This study utilized the H9c2 cardiomyocyte model to identify a sublethal concentration of Dox and investigate its impact on mitochondrial health using markers such as mitochondrial membrane potential (MMP), mitophagy initiation, and mitochondrial calcium dynamics. We examined the roles of and interactions between CaMKII, dynamin-related protein 1 (Drp1), and the mitochondrial calcium uniporter (MCU) in Dox-induced mitochondrial disruption using specific inhibitors, such as KN-93, Mdivi-1, and Ru360, respectively.

Results Exposure to a sublethal dose of Dox reduced the MMP red-to-green fluorescence ratio in H9c2 cells by 40.6% compared with vehicle, and increased the proportion of cells undergoing mitophagy from negligible levels compared with vehicle to 62.2%. Mitochondrial calcium levels also increased by 8.7-fold compared with

the vehicle group. Notably, the activation of CaMKII, particularly its phosphorylated form, was pivotal in driving these mitochondrial changes, as inhibition using KN-93 restored MMP and decreased mitophagy. However, inhibition of Drp1 and MCU functions had a limited impact on the observed mitochondrial disruptions.

Conclusion Sublethal administration of Dox is closely linked to CaMKII activation through phosphorylation, emphasizing its pivotal role in early mitochondrial disruption. These findings present a promising direction for developing therapeutic strategies that may alleviate the cardiotoxic effects of Dox, potentially increasing its clinical efficacy.

Key words CaMKII; doxorubicin; H9c2 cells; mitochondrial dysfunction; sublethal dose

Doxorubicin (Dox) presents a therapeutic paradox because, although it is a potent anthracycline chemotherapeutic agent, its utility is limited by pronounced, dose-dependent cardiotoxic effects.^{1, 2} This cardiotoxicity is often typified by cardiomyocyte death, a phenomenon that is intimately linked to mitochondrial dysfunction.^{3–6} Given the acute sensitivity of mitochondria to cellular disturbances,^{7, 8} exploring early mitochondrial disruptions in response to Dox is crucial and may present a prospect for innovative therapeutic interventions.

Although previous research has predominantly focused on lethal Dox doses,^{3, 6, 9} we hypothesized that investigating sublethal doses may allow examination of initial mitochondrial disruptions and the underlying mechanisms leading to Dox-induced cardiomyocyte death. In this context, the activation of calcium/calmodulin-dependent protein kinase II (CaMKII) by Dox, particularly through its autophosphorylation, warrants particular attention, given its implicated role in precipitating mitochondrial dysfunction.^{9–12} Dox has been shown to induce cytotoxicity through the generation of reactive oxygen species, which can target proteins and

Corresponding Author: Junichiro Miake, MD, PhD
jmiake@tottori-u.ac.jp

Received 2023 November 20

Accepted 2023 December 7

Online published 2024 January 4

Abbreviations: ANOVA, analysis of variance; CaMKII, Calcium/Calmodulin-dependent protein kinase II; DMSO, dimethyl sulfoxide; Dox, doxorubicin; Drp1, dynamin-related protein 1; Ex/Em, excitation/emission; FBS, fetal bovine serum; [Ca²⁺] mito, mitochondrial calcium; MCU, mitochondrial calcium uniporter; MMP, mitochondrial membrane potential; ns, not significant; pCaMKII, autophosphorylated calcium/calmodulin-dependent protein kinase II; PI, propidium iodide; PVDF, polyvinylidene fluoride; Thr, threonine

nucleic acids and induce damage in many different cellular compartments. While the paradigm of oxidation-induced CaMKII activation is well established,^{13–15} the current study examines CaMKII activation via autophosphorylation in relation to intracellular calcium modulation during sublethal Dox administration.^{10, 16, 17}

Mitophagy is regulated by calcium modulation¹⁸ and is essential for maintaining mitochondrial function, playing both adaptive^{19, 20} and potentially maladaptive⁶ roles under stress conditions. An increase in intramitochondrial calcium ($[Ca^{2+}]_{mito}$) can destabilize the mitochondrial membrane potential (MMP) and induce cell death.^{4, 11, 21} MMP is inextricably linked to ATP synthesis capability²² and serves as an early indicator of mitochondrial dysfunction.⁴ Dynamin-related protein 1 (Drp1), a target of CaMKII,²³ warrants further examination regarding its role in Dox-induced mitochondrial dysfunction during sublethal phases, as it plays a role in apoptosis regulated by changes in MMP. Therefore, Drp1 emerges as a central element in the investigation into the sublethal effects of Dox.

Utilizing the H9c2 cardiomyocyte model, this study aims to investigate the effects of sublethal Dox exposure on mitochondrial function, focusing on autophosphorylation-activated CaMKII (pCaMKII) and the interrelated dynamics of MMP, mitophagy, and calcium within the mitochondria,^{11, 12, 21, 22} with the goal of illuminating potential new therapeutic avenues.

MATERIALS AND METHODS

Cell culture

Embryonic rat heart-derived (H9c2) cells were cultured in high-glucose Dulbecco's Modified Eagle's Medium (Nacalai Tesque, Kyoto, Japan, Catalog no. 08458-16) supplemented with 10% fetal bovine serum (FBS) which has been heat-inactivated (Thermo Fisher Scientific, Waltham, MA, Catalog no. 10270-106). Cells were maintained at 37°C, 5% CO₂ in a humidified incubator. Growth medium was replaced every 48 hours. Upon reaching 70–80% confluence, cells were detached using a 0.25% trypsin-EDTA solution (Fujifilm Wako Pure Chemical Corporation, Osaka, Japan, Catalog no. 201-16945). To ensure consistent cellular behaviors, experiments were conducted using cells between passages 25–40.

Determination of sublethal dose of doxorubicin

To identify the sublethal dose of Dox, H9c2 cells were seeded at a density of 8.0×10^3 cells/well in 96-well plate on a culture medium supplemented with 10% FBS and allowed to adhere overnight. The next day, cells were then exposed to varying concentrations (0.1,

0.5, and 1.0 μ M) of Dox (Cayman Chemical Company, Ann Arbor, MI, Catalog no. 15007) dissolved in DMSO (Nacalai Tesque, Catalog no. 09659-14) for 24 hours. After exposure, cells were stained with 0.01 mg/mL propidium iodide (PI) solution (Dojindo Laboratories, Kumamoto, Japan, Catalog no. P378) and 50 μ M Hoechst 33342 (Hoechst) (Dojindo Laboratories, Catalog no. H342) in a light-protected environment. Using a fluorescence microscope (Keyence Corporation, Osaka, Japan, Catalog no. BZ-X710), images were captured from randomly selected fields of the well and analyzed using the FIJI (ImageJ) software. The number of PI-positive cells was then quantified and compared to the total count of Hoechst-positive cells.²⁴ A Dox concentration that resulted in less than 10% PI-positive cells were considered the sublethal dose.²⁵

Evaluation of mitochondrial membrane potential

H9c2 cells were seeded and treated with Dox as previously described. Specific cell groups received pretreatment with 5.0 μ M KN-93 (Cayman Chemical Company, Catalog no. 21472), 5.0 μ M Mdivi-1 (Selleck chemicals LLC., Houston, TX, Catalog no. S7162), or 5.0 μ M Ru360 (Merck KGaA., Darmstadt, Germany, Catalog no. 557440) two hours before and during the 24-hour Dox treatment. For the assay, cells were incubated with 2 μ M JC-1 dye (Dojindo Laboratories, Catalog no. MT09) for 30 minutes in a CO₂ incubator. Following incubation, cells were washed twice with warm culture medium without phenol red (Fujifilm Wako Pure Chemical Corporation, Catalog no. 048-33575) and fluorescence intensities of both red (JC-1 aggregates) and green (JC-1 monomers) were recorded using a fluorescence microplate reader (Tecan Group Ltd., Männedorf, Switzerland, Catalog no. INFINITE M200 PRO),²⁶ fluorescence intensity of Ex/Em = 535/590 nm and Ex/Em = 485/535 nm is determined for red and green, respectively. Alterations in the red and green fluorescence intensity indicated changes in the mitochondrial membrane potential. Measurements were taken every 45 seconds, a total of five times, and subsequently represented as a red-to-green fluorescence intensity ratio (R/G ratio). Cellular images were captured using a fluorescence microscope (Keyence Corporation Catalog no. BZ-X710).

Evaluation of mitophagy

To evaluate mitophagy, H9c2 cells were plated in 96-well plates and allowed to adhere overnight. Before Dox treatment, cells were incubated with 0.1 μ M Mitophagy Dye (Dojindo Laboratories, Catalog no. MD01) for 30 minutes in a CO₂ incubator. The Dox treatment, KN-93

and Mdivi-1 pre-treatment were subsequently carried out as previously described. After treatment, cells were washed and stained with 50 μM Hoechst to label the nuclei. After capturing the image using fluorescence microscopy, ImageJ software was used to analyze cells that display red (MtpHagy dye) fluorescence²⁷ and colocalized with blue (Hoechst) fluorescence, indicative of active mitophagy.

Evaluation of mitochondrial calcium

H9c2 cells were seeded and treated with Dox and were pre-treated with either 5.0 μM KN-93 or 5.0 μM Ru360 as described in previous sections. To measure $[\text{Ca}^{2+}]_{\text{mito}}$ levels, cells were loaded with a mixture of 2.5 μM dihydro-Rhod-2 AM with 0.02% Pluronic acid. This mixture was achieved by mixing Rhod-2 AM (Cayman Chemical Company, Catalog no. 19355) with Pluronic F-127 20% solution in DMSO (Biotium Inc., Fremont, CA, Catalog no. 59004) and add a small quantity of sodium borohydride (Merck KGaA., Catalog no. 213462) until the mixture turned transparent, prior adding to the cells. Following this, cells were incubated for 30 minutes in the dark. The fluorescence intensity was measured at 30-minute intervals before and after the Dox treatment. The difference in dihydro-Rhod-2 AM fluorescence levels corresponded to the $[\text{Ca}^{2+}]_{\text{mito}}$.²⁸

Western blotting

To analyze protein expression, H9c2 cells were lysed using cold RIPA buffer (Nacalai Tesque, Catalog no. 16488-34) supplemented with the inhibitors of protease (Roche diagnostics corporation, Basel, Switzerland, Catalog no. 11697498001) and phosphatase (Merck KGaA., Catalog no. P5726). Supernatant was collected after centrifugation and the protein concentration determined using the BCA Protein Assay Kit (Takara Bio Inc, Shiga, Japan, Catalog no. T9300A).²⁹ An equal amount of protein (10 μg) was subjected to SDS-PAGE and subsequently transferred onto PVDF membranes (Merck KGaA., Catalog no. IPVH00010). Membranes were blocked with 5% BSA (Merck KGaA., Catalog no. A9418) in TBS-T (Takara Bio Inc., Catalog no. T9300A-3) for 1 hour and subsequently incubated overnight at 4°C with primary antibodies: CaMKII-pThr286/Thr287 (Cell Signaling Technology Inc., Danvers, MA, Catalog no. 12716S) at a 1: 1000 dilution, CaMKII (Cell Signaling Technology Inc., Catalog no. 4436S) at a 1: 1000 dilution, and β -actin (Abcam plc, Cambridge, United Kingdom, Catalog no. ab20272) at a 1: 4000 dilution. Following a wash, the membranes were exposed to horseradish peroxidase-conjugated secondary antibodies (Cell Signaling Technology Inc.,

Catalog no. 7074S) for 1 hour at room temperature. Protein bands were visualized using Pierce™ ECL Plus western blotting substrate (Thermo Fisher Scientific, Catalog no. 32132) and ChemiDoc™ Touch MP imaging system (Bio-Rad, Hercules, CA).³⁰ The images were quantified using FIJI (ImageJ) software.³¹

Statistical analysis

Data are presented as mean \pm standard deviation (SD). Prior to analysis, the normality of all experimental data sets was verified. Subsequently, data sets underwent analysis using one-way ANOVA, followed by the Tukey post-hoc test for multiple group comparisons. A p-value of less than 0.05 was considered statistically significant. Analyses were performed using GraphPad Prism (Version 10.0.2, GraphPad software, Boston, MA).

RESULTS

Determination of the sublethal dose of doxorubicin in H9c2 cardiac cells

To determine a sublethal dose of Dox in H9c2 cardiac cells, cells were treated with vehicle or increasing doses of Dox for 24 hours. Cell viability was assessed by observing images and measuring the percentage of propidium iodide (PI)-positive cells relative to the total cell count, as determined by Hoechst staining (Fig. 1A).

In the vehicle group, PI-positive cells were not observed (0%, Fig. 1B). Following treatment with 0.1 μM Dox, 0%–4.7% of cells were PI-positive, which was not statistically significantly different when compared with the vehicle group (Fig. 1B). At a concentration of 0.5 μM Dox, the percentage of PI-positive cells rose to 4.2%–7.4% ($P < 0.05$, Fig. 1B). When treated with 1.0 μM Dox, cells exhibited a significant increase in the percentage of PI-positive cells, ranging from 19.5%–31.1% ($P < 0.01$, Fig. 1B).

Given our definition of a sublethal dose as one resulting in $< 10\%$ PI-positive cells, the 0.5 μM Dox treatment for 24 hours was selected for subsequent experiments with H9c2 cells (Fig. 1B).

Sublethal doses of doxorubicin decrease mitochondrial membrane potential in H9c2 cells

The JC-1 dye assay was used to assess the effects of a sublethal dose of Dox on MMP, an early indicator of mitochondrial health in H9c2 cells. A decrease in the red-to-green ratio (R/G ratio) indicates mitochondrial depolarization and dysfunction. H9c2 cells were treated with the same Dox concentrations as described earlier (Fig. 1C). The vehicle group exhibited an R/G ratio of 3.2. Treatment with 0.1 μM Dox resulted in a 21.9% reduction in the R/G ratio to 2.5 ($P < 0.05$, Fig. 1D). With

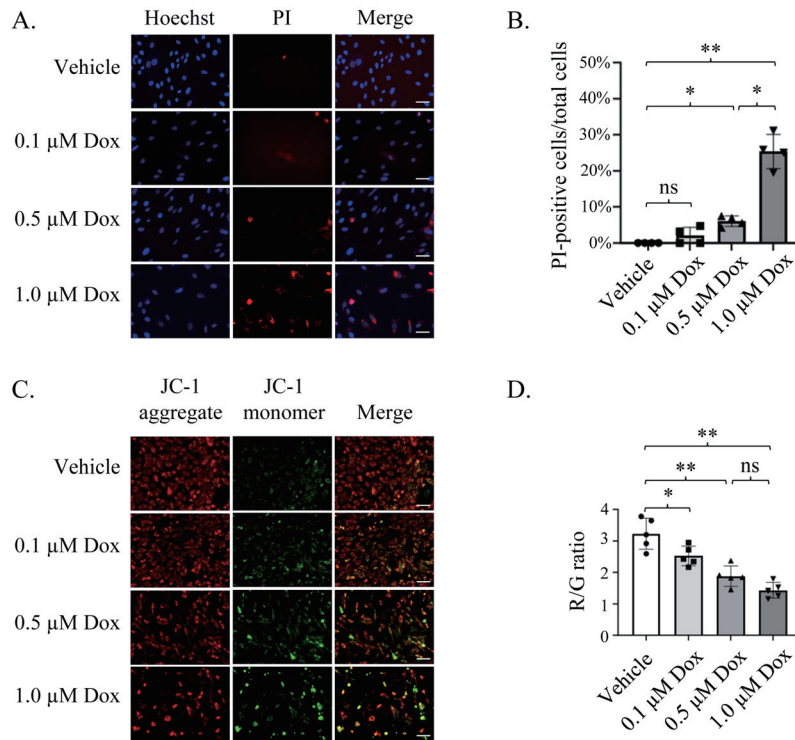


Fig. 1. The effect of sublethal doxorubicin on mitochondrial membrane potential. **(A)** H9c2 cells (8.0×10^3 cells/well in 96-well plate) were incubated with 0.1, 0.5, or 1.0 μM Dox or the vehicle group for 24 hours. Cell viability was detected by PI (red) staining. **(B)** The number of dead cells was quantified and is represented as the ratio of PI-positive cells (red) to Hoechst 33342-positive cells (blue) ($n = 4$). **(C)** H9c2 cells were treated with 0.1, 0.5, or 1.0 μM Dox or the vehicle group for 24 hours. Afterward, cells were incubated with 2.0 μM JC-1 dye for 30 minutes to evaluate the mitochondrial membrane potential (representative image). **(D)** The mitochondrial membrane potential was measured using a microplate reader and is represented as the R/G ratio ($n = 5$). Data are mean \pm SD, scale bar = 100 μm , $*P < 0.05$; $**P < 0.01$, significantly different as indicated.

0.5 μM Dox, the R/G ratio decreased to 1.9, a 40.6% decrease from the vehicle ($P < 0.01$, Fig. 1D). At 1.0 μM Dox, the R/G ratio further decreased to 1.4, a 56.3% decrease from the vehicle ($P < 0.01$, Fig. 1D). These results indicate a dose-dependent decrease in MMP in H9c2 cells after Dox treatment, underscoring its potential impact on mitochondrial function.

Phosphorylation-activated CaMKII mediates mitochondrial dysfunction induced by a sublethal dose of doxorubicin

To evaluate the molecular mechanisms resulting in the observed mitochondrial dysfunction induced by sublethal Dox treatment, we focused on the role of CaMKII. This kinase is activated via autophosphorylation upon binding with activated calmodulin.¹⁶ Specifically, we investigated whether calcium-induced autophosphorylation of CaMKII potentiates mitochondrial dysfunction in H9c2 cells treated with sublethal Dox by using western blot analysis with an antibody specific to CaMKII phosphorylated at Thr286/287. As shown in Fig. 2A, the

levels of pCaMKII, when normalized to total CaMKII, increased from 1.0 in the vehicle-treated group to 2.0 in the Dox-treated group ($P < 0.05$). This increase in pCaMKII was abolished by the CaMKII inhibitor KN-93 ($P < 0.05$), which inhibits the interaction between calmodulin and CaMKII.³² This underscores that the observed elevation in pCaMKII in response to sublethal Dox occurs through calcium-mediated signaling.

Evaluation of MMP by R/G ratio using JC-1 dye following treatment with KN-93 demonstrated that the R/G ratio was diminished by 42.0%, from 3.1 in the vehicle group to 1.8 upon 0.5 μM Dox treatment ($P < 0.01$, Fig. 2B). This reduction was entirely restored to the level of the vehicle group in cells that were co-treated with KN-93 ($P < 0.01$, Fig. 2C). These findings indicate that phosphorylation-activated CaMKII is required for the mitochondrial dysfunction observed in H9c2 cells treated with sublethal Dox.

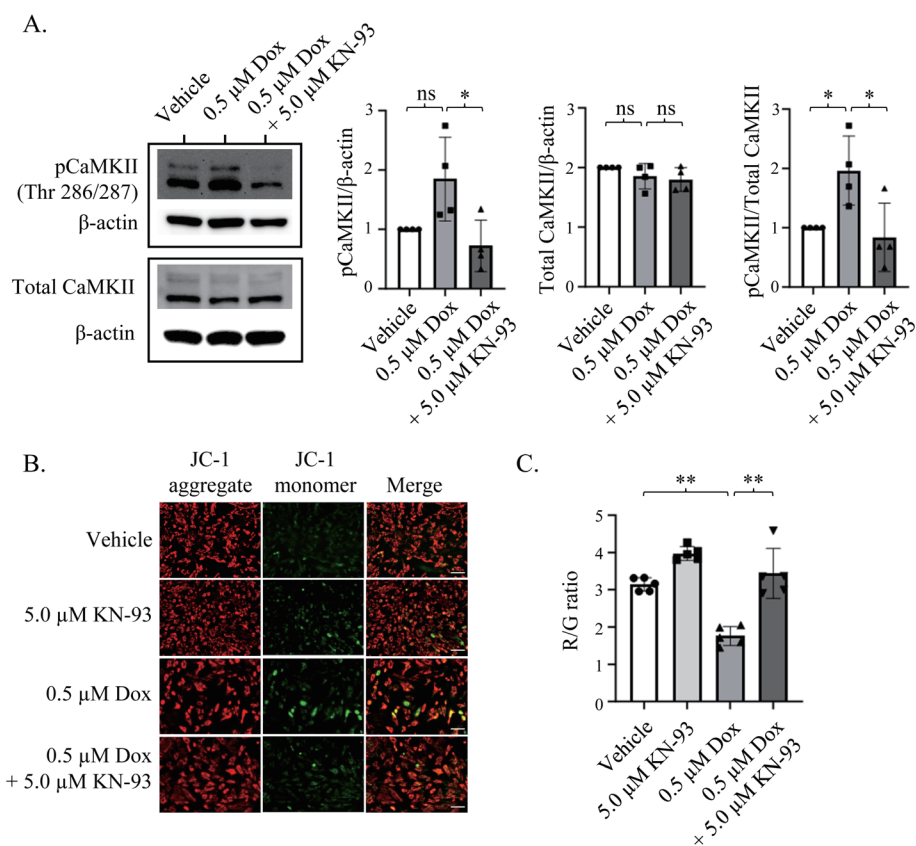


Fig. 2. Role of CaMKII phosphorylation in mitochondrial membrane potential reduction induced by a sublethal dose of doxorubicin. (A) Western blot analysis was performed on proteins harvested from H9c2 cells seeded at a density of 3.0×10^5 cells/well in 6-well plate. Total CaMKII and phosphorylated CaMKII levels were normalized with corresponding β -actin and represented as the ratio of phosphorylated CaMKII to Total CaMKII. Dox treatment significantly increased the phosphorylation level of CaMKII, while KN-93 pre-treatment prevented this Dox-induced CaMKII activation ($n = 4$). (B) H9c2 cells (8.0×10^3 cells/well in 96-well plate) were treated with 0.5 μ M Dox or vehicle group for 24 hours, with or without a 5.0 μ M KN-93 pre-treatment for two hours. Subsequently, cells were incubated with 2.0 μ M JC-1 dye for 30 minutes to evaluate the MMP. KN-93 pre-treatment effectively prevented the Dox-induced MMP reduction (Representative image). (C) MMP was assessed using a microplate reader and is represented as the R/G ratio ($n = 5$). Data are shown as mean \pm SD; scale bar = 100 μ m. * $P < 0.05$; ** $P < 0.01$, indicating significant differences as marked.

Sublethal doses of doxorubicin induce adaptive mitophagy via CaMKII activation

Mitophagy is a selective form of autophagy targeting mitochondria that can perform both adaptive (protective) as well as maladaptive (pathological) roles. Though initially identified as a protective response, excessive mitochondrial fission, particularly as mediated by the protein Drp1, may lead to cytotoxic effects. As Drp1 has been shown to be phosphorylated by CaMKII,²³ we explored whether the elevated levels of pCaMKII observed in response to sublethal concentrations of Dox led to increased mitophagy.

Using the Mtpagy dye, which accumulates in intact mitochondria and emits enhanced fluorescence upon mitochondrial fusion with lysosomes during mitophagy, we assessed mitophagy levels in response to Dox in a dose-dependent manner (Fig. 3A). In the

vehicle-treated group, only 0.1% of the cells were mitophagy-positive. Treatment with 0.1 μ M Dox increased this to 3.5%; however, this increase was not statistically significant (Fig. 3B). A significant rise was observed with the sublethal dose of 0.5 μ M Dox, where 62.2% of cells were mitophagy-positive ($P < 0.01$, Fig. 3B). In contrast, at 1.0 μ M Dox, which is the lethal dose for the cells as shown in Figs. 1A and B, this percentage surged to 97.4% ($P < 0.01$, Fig. 3B).

To evaluate the role of pCaMKII in Dox-induced mitophagy, H9c2 cells were treated with the CaMKII inhibitor KN-93 (Fig. 3C). In the vehicle-treated group, 1.9% of cells showed mitophagy. This proportion significantly increased to 58.1% after treatment with 0.5 μ M Dox ($P < 0.01$, Fig. 3D). However, co-treatment with 5.0 μ M KN-93, an inhibitor of autophosphorylation-activated CaMKII, significantly reduced the mitophagy

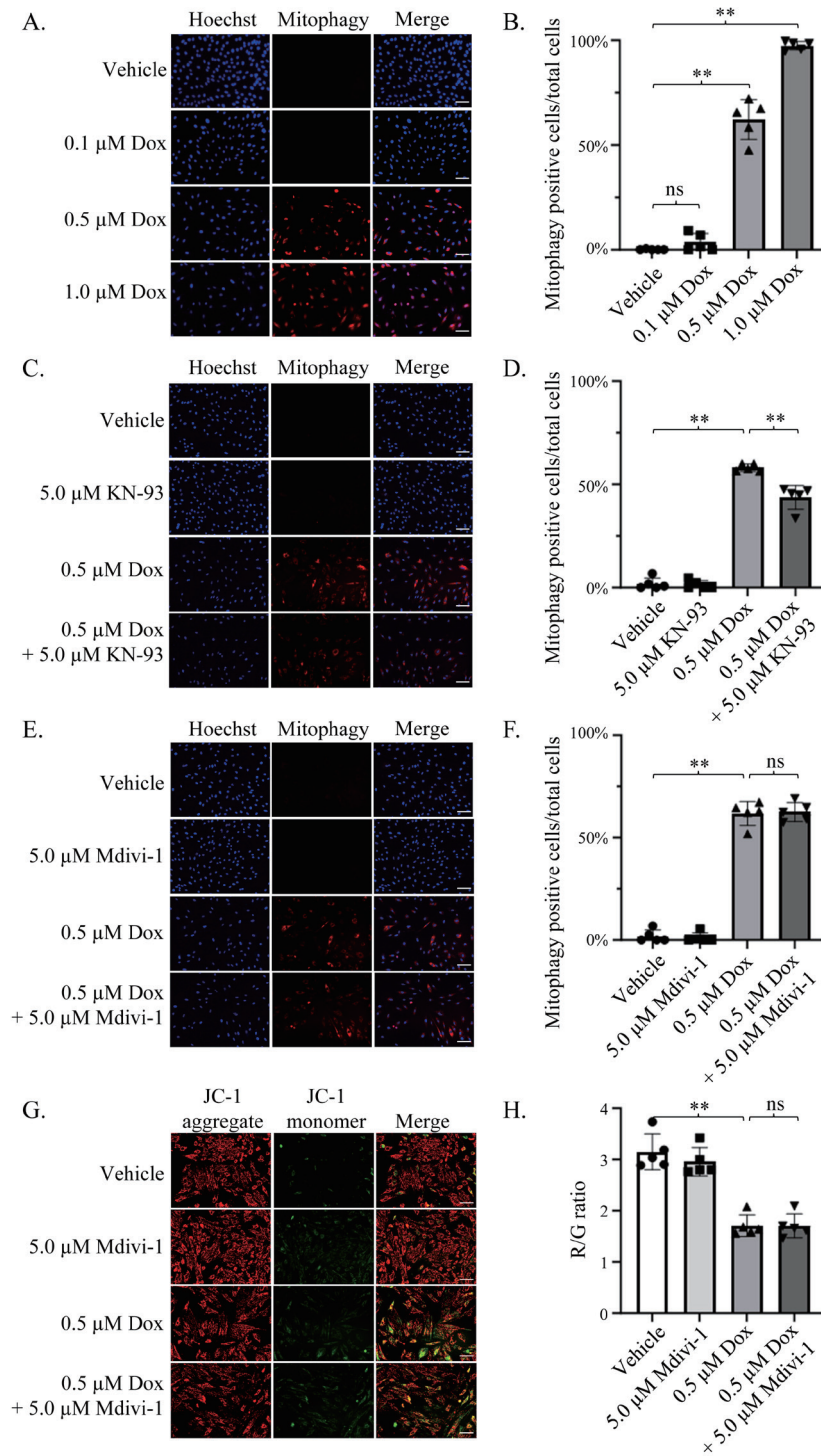


Fig. 3. Role of CaMKII in adaptive mitophagy following a sublethal dose of doxorubicin exposure. (A) H9c2 cells (8.0×10^3 cells/well in 96-well plate) were treated with varying concentrations of Dox for 24 hours, showing a dose-dependent increase in mitophagic activity. (B) Quantification of cells undergoing mitophagy, represented as the ratio of mitophagy-positive staining (red) to Hoechst 33342-positive staining (blue) ($n = 5$). (C) KN-93 pre-treatment (5.0 μM) led to a reduction in Dox-induced mitophagy ($n = 5$). (D) Quantitative analysis of the cells from (C) showing the mitophagy ratio. (E) Mdivi-1 pre-treatment (5.0 μM) did not affect Dox-induced mitophagy ($n = 5$). (F) Quantitative analysis of the cells from (E) showing the mitophagy ratio. (G) Representative image of H9c2 cells (8.0×10^3 cells/well in 96-well plate) treated with 0.5 μM Dox or vehicle group for 24 hours, with or without Mdivi-1 (5.0 μM) pre-treatment. Mdivi-1 did not prevent the Dox-induced reduction in MMP (representative image). (H) Quantitative analysis of MMP, represented as the R/G ratio ($n = 5$). Data are shown as mean \pm SD; scale bar = 100 μm . * $P < 0.05$; ** $P < 0.01$, indicating significant differences as marked.

level to 43.7% ($P < 0.01$, Fig. 3D).

Considering the significant reduction in mitophagy after KN-93 treatment, we further explored whether Drp1, a downstream target molecule of CaMKII, played a role in this process. For this, we used Mdivi-1, a specific inhibitor of Drp1 (Fig. 3E). In the vehicle-treated group, 1.9% of cells were mitophagy-positive (Fig. 3F). Treatment with 0.5 μM Dox led to a significant increase in mitophagy-positive cells, to 61.8% ($P < 0.01$, Fig. 3F). Notably, the addition of 5.0 μM Mdivi-1 did not lead to a significant reduction in mitophagy levels, with 62.6% of cells still being mitophagy-positive (Fig. 3F).

Lastly, we aimed to investigate the role of Drp1 in the MMP reduction induced by a sublethal dose of Dox, using Mdivi-1 and the JC-1 dye as an MMP indicator (Fig. 3G). The R/G ratio significantly decreased from 3.2 in the vehicle group to 1.7 after 0.5 μM Dox treatment ($P < 0.01$, Fig. 3H). The addition of Mdivi-1 did not alter this ratio, maintaining it at 1.7 (Fig. 3H).

Mitochondrial calcium uptake is required for sublethal doxorubicin-induced mitochondrial dysfunction

The importance of mitochondrial calcium ($[\text{Ca}^{2+}]_{\text{mito}}$) levels in cellular health is well established. Dysregulation of these calcium levels, especially excessive $[\text{Ca}^{2+}]_{\text{mito}}$, can impair mitochondrial functions including ATP synthesis, and may even trigger apoptosis. The mitochondrial calcium uniporter (MCU) is responsible for calcium uptake into the mitochondria^{18, 33} and is known to be a phosphorylation target of activated CaMKII.¹¹ As we observed that phosphorylation of CaMKII was increased in response to sublethal Dox, we aimed to determine whether altered $[\text{Ca}^{2+}]_{\text{mito}}$ levels, mediated by the MCU, contribute to the mitochondrial dysfunction observed with sublethal Dox treatment.

To address this, we first assessed the $[\text{Ca}^{2+}]_{\text{mito}}$ levels in H9c2 cells treated with Dox by using Rhod-2 AM dye, a fluorescent indicator that is sensitive to $[\text{Ca}^{2+}]_{\text{mito}}$. Using Rhod-2 AM, we found a statistically significant increase in $[\text{Ca}^{2+}]_{\text{mito}}$, to 83.4, representing an 8.7-fold increase observed upon 0.5 μM Dox treatment compared with vehicle which is detected at 9.6 (Fig. 4A). With 1.0 μM Dox treatment, the increase in $[\text{Ca}^{2+}]_{\text{mito}}$ increased further to 232.8, representing a 24.3-fold increase over the level of the vehicle group ($P < 0.01$, Fig. 4A).

To delineate the involvement of autophosphorylation-activated CaMKII in the increased $[\text{Ca}^{2+}]_{\text{mito}}$ levels observed following Dox treatment, H9c2 cells were pre-treated with KN-93 inhibitor. Interestingly, KN-93 did not attenuate the elevated $[\text{Ca}^{2+}]_{\text{mito}}$ levels seen in

response to sublethal doses of Dox. The fluorescence intensity of the vehicle group was measured at 10.2, and with 0.5 μM Dox treatment, a 7.2-fold increase of fluorescence intensity to 73.2 was detected ($P < 0.01$). In the group treated with both 0.5 μM Dox and KN-93, the fluorescence intensity was measured at 80.7, showing a non-statistically significant change compared to the Dox-treated group (Fig. 4B) and suggesting that autophosphorylation-activated CaMKII might not regulate $[\text{Ca}^{2+}]_{\text{mito}}$ in response to Dox.

As the MCU has been shown to play a role in regulating $[\text{Ca}^{2+}]_{\text{mito}}$, we evaluated the impact of Ru360, a specific inhibitor of the MCU, on $[\text{Ca}^{2+}]_{\text{mito}}$. Ru360 did not diminish the increased $[\text{Ca}^{2+}]_{\text{mito}}$ levels induced by sublethal Dox. In the vehicle group, the fluorescence intensity was measured at 12.7. Following treatment with 0.5 μM Dox, an increase of 6.9-fold to 88.1 was observed ($P < 0.05$). Pre-treatment with Ru360 resulted in a fluorescence intensity of 92.7, which was non-significant compared with the Dox-treated group (Fig. 4C).

Finally, since sublethal concentrations of Dox were shown to decrease MMP as well as increase $[\text{Ca}^{2+}]_{\text{mito}}$, the effect of inhibiting the MCU on MMP in response to Dox was assessed (Fig. 4D). Inhibition of the MCU with Ru360 did not ameliorate the reduction in MMP induced by sublethal Dox. The R/G ratio of the vehicle group was 3.1; following 0.5 μM Dox treatment, the R/G ratio decreased to 1.7, representing a 45.2% decline ($P < 0.01$). In the Ru360 pre-treated group, the R/G ratio was 2.0, which was non-significantly different compared with the Dox-treated group (Fig. 4E). This indicates that elevated $[\text{Ca}^{2+}]_{\text{mito}}$ in response to Dox may not be the primary mechanism by which Dox decreases MMP and disrupts mitochondrial function.

DISCUSSION

Dox, while widely recognized for its potent anticancer properties, simultaneously poses a significant clinical challenge because of its dose-dependent cardiotoxic effects, which often progress to heart failure. To elucidate the mechanisms underlying Dox-induced cardiomyopathy, we evaluated the sublethal effects of Dox exposure in a cardiomyocyte model. We hypothesized that early mitochondrial dysfunction mediated by autophosphorylation-activated CaMKII plays a pivotal role in controlling the cellular response to Dox. The data from the current study substantiate this hypothesis, revealing intricate pathways that intertwine mitophagy and mitochondrial calcium dynamics, as depicted in Figure 5.

Having established 0.5 μM Dox as a sublethal

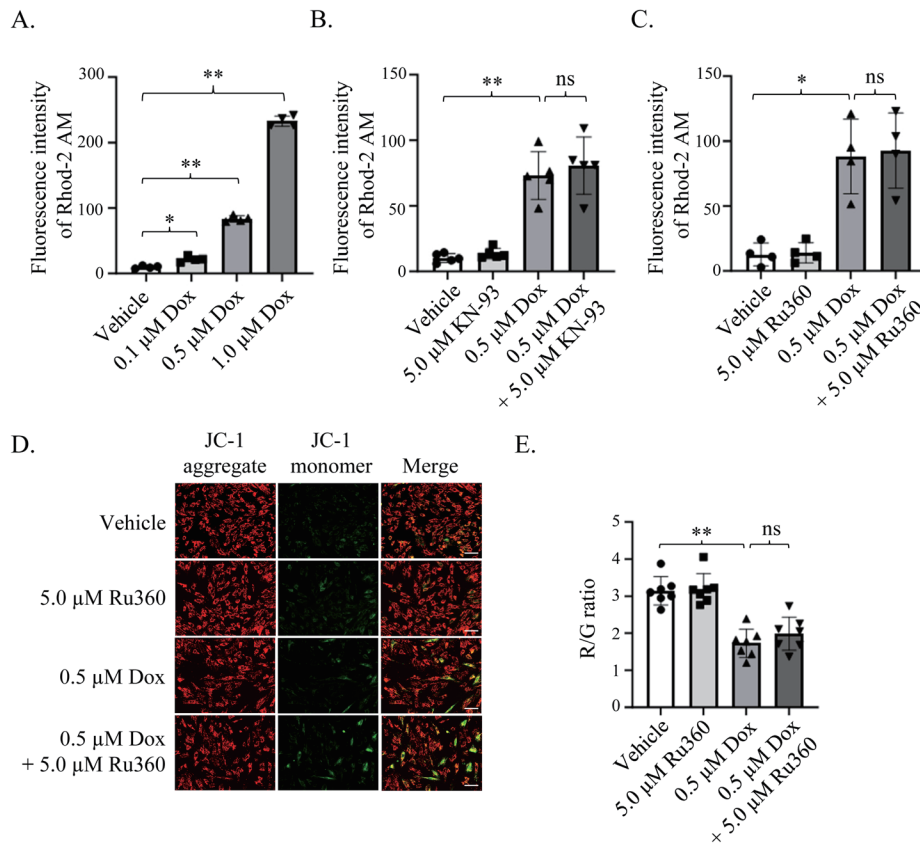


Fig. 4. Role of CaMKII in mitochondrial calcium dynamics upon sublethal doxorubicin exposure. $[Ca^{2+}]_{\text{mito}}$ was measured using dihydro-rhod-2 AM. (A) H9c2 cells treated with 0.1, 0.5, or 1.0 μM Dox display increased $[Ca^{2+}]_{\text{mito}}$. Data, representing the fluorescence intensity difference before and 30 min post Dox treatment, were collected using a microplate reader. ($n = 4$). (B) Pre-treatment with 5.0 μM KN-93 for 2 hours did not mitigate the Dox-induced rise in $[Ca^{2+}]_{\text{mito}}$. ($n = 5$). (C) Similarly, Ru360 pre-treatment did not avert the Dox-induced surge in $[Ca^{2+}]_{\text{mito}}$. ($n = 4$). (D) H9c2 cells were treated with 0.5 μM Dox for 24 hours, with or without a 2-hour pre-treatment using 5.0 μM Ru360 (MCU inhibitor). Subsequent incubation with 2.0 μM JC-1 dye for 30 min was conducted to assess MMP. (E) Ru360 pre-treatment failed to prevent the Dox-induced MMP decline, with MMP data measured via a microplate reader and presented as the R/G ratio ($n = 7$). Data are expressed as mean \pm SD; scale bar = 100 μm . * $P < 0.05$; ** $P < 0.01$, indicating significant differences where noted.

dose in H9c2 cells, we next identified a crucial phase in which the cells, although not lethally compromised, have been exposed to substantial stress. Mitochondrial perturbations serve as early events,⁴ but may potentially lead to overt cardiomyopathy, and thus, could act as early indicators for proactive therapeutic interventions. We observed a significant decrease in the R/G ratio of JC-1 dye, a marker of reduced MMP, following Dox exposure, indicating pronounced mitochondrial dysfunction even at sublethal doses of Dox. While this detrimental impact of Dox on mitochondrial function aligns with findings from previous studies,^{3, 4, 6} in the current study, co-treatment with the CaMKII inhibitor KN-93 restored the amelioration of the R/G ratio, demonstrating the novel finding that autophosphorylation-activated CaMKII is required for the observed Dox-mediated decrease in MMP. Although oxidation-activated CaMKII

has been shown to play roles in various cellular dynamics,^{13–15} this study demonstrates that pCaMKII is pivotal in mediating Dox-triggered mitochondrial disruptions. This finding highlights the potential utility of inhibiting CaMKII phosphorylation as a strategy to mitigate Dox-induced mitochondrial disruption.

In response to a decrease in MMP, mitophagy may occur, as has been demonstrated in various studies.^{7, 19, 22} Sublethal Dox increased the percentage of cells undergoing mitophagy (Fig. 3), which aligns with the findings of Bisaccia et al. and Kim and Lemasters, suggesting that mitophagy acts as a cellular defense mechanism against stress.^{7, 19} This response to stress could be interpreted as an adaptive mechanism to counterbalance Dox-induced alterations in mitochondrial dynamics.²⁰ Our findings indicate that the inhibition of pCaMKII by KN-93 significantly reduced Dox-induced

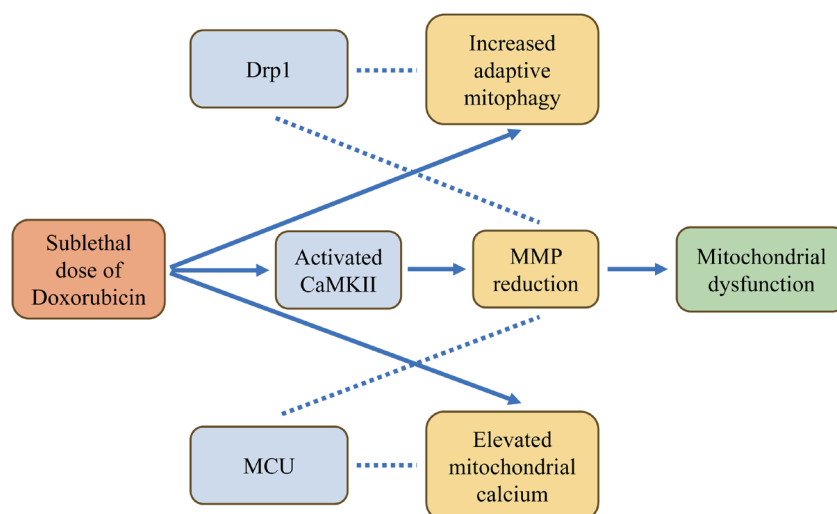


Fig. 5. CaMKII activation underpins mitochondrial dysfunction induced by sublethal Dox exposure. Sublethal Dox exposure results in noticeable mitochondrial dysfunction, evident through a decline in MMP. This is accompanied by an uptick in adaptive mitophagy and elevated $[Ca^{2+}]$ mito. Our findings pinpoint CaMKII activation as the primary driver behind the Dox-induced MMP reduction. The surge in mitophagy post-Dox exposure was not attributed to activated Drp1, suggesting it is an adaptive response to the diminished MMP rather than maladaptive mitophagy. The rise in mitochondrial calcium is independent of both CaMKII activation and its downstream effector, MCU. Solid arrows denote direct relationships observed in our study, while dashed lines without arrowheads signify previously known associations that, though pharmacologically confirmed, did not influence in our experimental context.

mitophagy, suggesting a role of pCaMKII in this process. In contrast, inhibition of Drp1 with Mdivi-1 did not lead to a significant reduction in mitophagy levels, indicating that the role of Drp1 in Dox-induced mitophagy might be more complex or context-specific than previously anticipated.

The observed increase in $[Ca^{2+}]$ mito following sublethal Dox exposure suggests that, despite the well-characterized role of calcium dysregulation as a pivotal cellular stress factor,⁴ this increase occurred independently of autophosphorylation-activated CaMKII and the MCU, leading to additional questions. Further analysis of potentially more intricate and alternative calcium regulatory mechanisms is required, which merits further exploration.^{12, 33, 34}

Destabilization of MMP disrupts ATP synthesis and, consequently, the electromechanical functionality of cardiomyocytes through disrupted calcium homeostasis.^{7, 22} Given the elevated energy demands of the heart,^{7, 22} even a minor deviation in mitochondrial functionality could cascade into cellular dysfunction, affecting contractility and rhythm to varying degrees. While our study centered on early mitochondrial disturbances, the path from mitochondrial dysfunction to observable cardiomyopathy is not well established and requires further investigation.

The current study has certain limitations. Notably, the focus was on *in vitro* models, which may not

accurately recapitulate the *in vivo* microenvironment and may overlook the dynamics of cell-to-cell interactions and systemic responses.⁹ Moreover, the reliance of this study on specific molecular inhibitors to interrogate mitochondrial mechanisms of sublethal Dox concentrations might obscure potential, as-yet unidentified, components within a complex cellular signaling network that could impact cardiomyocyte toxicity.

In conclusion, our study reinforces the multifaceted and intricate cellular responses elicited by Dox; in particular, highlighting the impact of Dox on early mitochondrial dysfunction and the pivotal roles of pCaMKII, mitophagy, and mitochondrial calcium dynamics. Understanding how these pathways intersect may lay the foundation for evolving therapeutic strategies. By extension, understanding how Dox impacts mitochondrial dynamics may influence the approach toward managing Dox-induced cardiomyopathy, potentially altering the therapeutic landscape and improving patient outcomes.

The authors declare no conflict of interest.

REFERENCES

- Cardinale D, Colombo A, Bacchiani G, Tedeschi I, Meroni CA, Veglia F, et al. Early detection of anthracycline cardiotoxicity and improvement with heart failure therapy. *Circulation*. 2015;131:1981-8. DOI: [10.1161/CIRCULATIONAHA.114.013777](https://doi.org/10.1161/CIRCULATIONAHA.114.013777), PMID: 25948538

- 2 Swain SM, Whaley FS, Ewer MS. Congestive heart failure in patients treated with doxorubicin. *Cancer*. 2003;97:2869-79. DOI: 10.1002/cncr.11407, PMID: 12767102
- 3 Toda N, Sato T, Muraoka M, Lin D, Saito M, Li G, et al. Doxorubicin induces cardiomyocyte death owing to the accumulation of dysfunctional mitochondria by inhibiting the autophagy fusion process. *Free Radic Biol Med*. 2023;195:47-57. DOI: 10.1016/j.freeradbiomed.2022.12.082, PMID: 36566798
- 4 Kuznetsov AV, Margreiter R, Amberger A, Saks V, Grimm M. Changes in mitochondrial redox state, membrane potential and calcium precede mitochondrial dysfunction in doxorubicin-induced cell death. *Biochim Biophys Acta Mol Cell Res*. 2011;1813:1144-52. DOI: 10.1016/j.bbamcr.2011.03.002, PMID: 21406203
- 5 Gottlieb E, Armour SM, Harris MH, Thompson CB. Mitochondrial membrane potential regulates matrix configuration and cytochrome c release during apoptosis. *Cell Death Differ*. 2003;10:709-17. DOI: 10.1038/sj.cdd.4401231, PMID: 12761579
- 6 Catanzaro MP, Weiner A, Kaminaris A, Li C, Cai F, Zhao F, et al. Doxorubicin-induced cardiomyocyte death is mediated by unchecked mitochondrial fission and mitophagy. *FASEB J*. 2019;33:11096-108. DOI: 10.1096/fj.201802663R, PMID: 31291545
- 7 Bisaccia G, Ricci F, Gallina S, Di Baldassarre A, Ghinassi B. Mitochondrial dysfunction and heart disease: critical appraisal of an overlooked association. *Int J Mol Sci*. 2021;22:614. DOI: 10.3390/ijms22020614, PMID: 33435429
- 8 Kim CW, Choi KC. Effects of anticancer drugs on the cardiac mitochondrial toxicity and their underlying mechanisms for novel cardiac protective strategies. *Life Sci*. 2021;277:119607. DOI: 10.1016/j.lfs.2021.119607, PMID: 33992675
- 9 Tscheschner H, Meinhardt E, Schlegel P, Jungmann A, Lehmann LH, Müller OJ, et al. CaMKII activation participates in doxorubicin cardiotoxicity and is attenuated by moderate GRP78 overexpression. *PLoS One*. 2019;14:e0215992. DOI: 10.1371/journal.pone.0215992, PMID: 31034488
- 10 Sag CM, Köhler AC, Anderson ME, Backs J, Maier LS. CaMKII-dependent SR Ca leak contributes to doxorubicin-induced impaired Ca handling in isolated cardiac myocytes. *J Mol Cell Cardiol*. 2011;51:749-59. DOI: 10.1016/j.jymcc.2011.07.016, PMID: 21819992
- 11 Joiner MA, Koval OM, Li J, He BJ, Allamargot C, Gao Z, et al. CaMKII determines mitochondrial stress responses in heart. *Nature*. 2012;491:269-73. DOI: 10.1038/nature11444, PMID: 23051746
- 12 Luczak ED, Wu Y, Granger JM, Joiner MA, Wilson NR, Gupta A, et al. Mitochondrial CaMKII causes adverse metabolic reprogramming and dilated cardiomyopathy. *Nat Commun*. 2020;11:4416. DOI: 10.1038/s41467-020-18165-6, PMID: 32887881
- 13 Erickson JR, Joiner MA, Guan X, Kutschke W, Yang J, Oddis CV, et al. A dynamic pathway for calcium-independent activation of CaMKII by methionine oxidation. *Cell*. 2008;133:462-74. DOI: 10.1016/j.cell.2008.02.048, PMID: 18455987
- 14 Yang Y, Jiang K, Liu X, Qin M, Xiang Y. CaMKII in Regulation of Cell Death During Myocardial Reperfusion Injury. *Front Mol Biosci*. 2021;8:668129. DOI: 10.3389/fmolb.2021.668129, PMID: 34141722
- 15 Zhang Y, Do DC, Hu X, Wang J, Zhao Y, Mishra S, et al. CaMKII oxidation regulates cockroach allergen-induced mitophagy in asthma. *J Allergy Clin Immunol*. 2021;147:1464-1477.e11. DOI: 10.1016/j.jaci.2020.08.033, PMID: 32920093
- 16 Erickson JR. Mechanisms of CaMKII activation in the heart. *Front Pharmacol*. 2014;5:59. DOI: 10.3389/fphar.2014.00059, PMID: 24765077
- 17 Ikeda S, Matsushima S, Okabe K, Ikeda M, Ishikita A, Tadokoro T, et al. Blockade of L-type Ca²⁺ channel attenuates doxorubicin-induced cardiomyopathy via suppression of CaMKII-NF-κB pathway. *Sci Rep*. 2019;9:9850. DOI: 10.1038/s41598-019-46367-6, PMID: 31285514
- 18 Yu Z, Chen R, Li M, Yu Y, Liang Y, Han F, et al. Mitochondrial calcium uniporter inhibition provides cardioprotection in pressure overload-induced heart failure through autophagy enhancement. *Int J Cardiol*. 2018;271:161-8. DOI: 10.1016/j.ijcard.2018.05.054, PMID: 29803339
- 19 Kim I, Lemasters JJ. Mitochondrial degradation by autophagy (mitophagy) in GFP-LC3 transgenic hepatocytes during nutrient deprivation. *Am J Physiol Cell Physiol*. 2011;300:C308-17. DOI: 10.1152/ajpcell.00056.2010, PMID: 21106691
- 20 Kim I, Lemasters JJ. Mitophagy selectively degrades individual damaged mitochondria after photoirradiation. *Antioxid Redox Signal*. 2011;14:1919-28. DOI: 10.1089/ars.2010.3768, PMID: 21126216
- 21 Briston T, Roberts M, Lewis S, Powney B, M Staddon J, Szabadkai G, et al. Mitochondrial permeability transition pore: sensitivity to opening and mechanistic dependence on substrate availability. *Sci Rep*. 2017;7:10492. DOI: 10.1038/s41598-017-10673-8, PMID: 28874733
- 22 Zorova LD, Popkov VA, Plotnikov EY, Silachev DN, Pevzner IB, Jankauskas SS, et al. Mitochondrial membrane potential. *Anal Biochem*. 2018;552:50-9. DOI: 10.1016/j.ab.2017.07.009, PMID: 28711444
- 23 Xu S, Wang P, Zhang H, Gong G, Gutierrez Cortes N, Zhu W, et al. CaMKII induces permeability transition through Drp1 phosphorylation during chronic β-AR stimulation. *Nat Commun*. 2016;7:13189. DOI: 10.1038/ncomms13189, PMID: 27739424
- 24 Pijuan J, Barceló C, Moreno DF, Maiques O, Sisó P, Martí RM, et al. *In vitro* Cell Migration, Invasion, and Adhesion Assays: From Cell Imaging to Data Analysis. *Front Cell Dev Biol*. 2019;7:107. DOI: 10.3389/fcell.2019.00107, PMID: 31259172
- 25 Kawalec P, Martens MD, Field JT, Mughal W, Caymo AM, Chapman D, et al. Differential impact of doxorubicin dose on cell death and autophagy pathways during acute cardiotoxicity. *Toxicol Appl Pharmacol*. 2022;453:116210. DOI: 10.1016/j.taap.2022.116210, PMID: 36028075
- 26 Mizusawa N, Harada N, Iwata T, Ohigashi I, Itakura M, Yoshimoto K. Identification of protease serine S1 family member 53 as a mitochondrial protein in murine islet beta cells. *Islets*. 2022;14:1-13. DOI: 10.1080/19382014.2021.1982325, PMID: 34636707
- 27 Inoue R, Tsuno T, Togashi Y, Okuyama T, Sato A, Nishiyama K, et al. Uncoupling protein 2 and aldolase B impact insulin release by modulating mitochondrial function and Ca. *iScience*. 2022;25:104603. PMID: 35800776
- 28 Nakagawa C, Suzuki-Karasaki M, Suzuki-Karasaki M, Ochiai T, Suzuki-Karasaki Y. The Mitochondrial Ca²⁺ Overload via Voltage-Gated Ca²⁺ Entry Contributes to an Anti-Melanoma Effect of Diallyl Trisulfide. *Int J Mol Sci*. 2020;21:491. DOI: 10.3390/ijms21020491, PMID: 31940976

- 29 Cortés-Ríos J, Zárate AM, Figueroa JD, Medina J, Fuentes-Lemus E, Rodríguez-Fernández M, et al. Protein quantification by bicinchoninic acid (BCA) assay follows complex kinetics and can be performed at short incubation times. *Anal Biochem.* 2020;608:113904. DOI: [10.1016/j.ab.2020.113904](https://doi.org/10.1016/j.ab.2020.113904), PMID: [32800701](https://pubmed.ncbi.nlm.nih.gov/32800701/)
- 30 Okamura A, Miake J, Tomomori T, Takami A, Sawano T, Kato M, et al. Thrombin induces a temporal biphasic vascular response through the differential phosphorylation of endothelial nitric oxide synthase via protease-activated receptor-1 and protein kinase C. *J Pharmacol Sci.* 2022;148:351-7. DOI: [10.1016/j.jphs.2022.02.001](https://doi.org/10.1016/j.jphs.2022.02.001), PMID: [35300809](https://pubmed.ncbi.nlm.nih.gov/35300809/)
- 31 Gallo-Oller G, Ordoñez R, Dotor J. A new background subtraction method for Western blot densitometry band quantification through image analysis software. *J Immunol Methods.* 2018;457:1-5. DOI: [10.1016/j.jim.2018.03.004](https://doi.org/10.1016/j.jim.2018.03.004), PMID: [29522776](https://pubmed.ncbi.nlm.nih.gov/29522776/)
- 32 Wong MH, Samal AB, Lee M, Vlach J, Novikov N, Niedziela-Majka A, et al. The KN-93 Molecule Inhibits Calcium/Calmodulin-Dependent Protein Kinase II (CaMKII) Activity by Binding to Ca²⁺/CaM. *J Mol Biol.* 2019;431:1440-59. DOI: [10.1016/j.jmb.2019.02.001](https://doi.org/10.1016/j.jmb.2019.02.001), PMID: [30753871](https://pubmed.ncbi.nlm.nih.gov/30753871/)
- 33 Yamada A, Watanabe A, Yamamoto T. Regulatory mechanisms of mitochondrial calcium uptake by the calcium uniporter complex. *Biophys Physicobiol.* 2023;20:e200004. DOI: [10.2142/biophysico.bppb-v20.0004](https://doi.org/10.2142/biophysico.bppb-v20.0004), PMID: [37234846](https://pubmed.ncbi.nlm.nih.gov/37234846/)
- 34 Nickel AG, Kohlhaas M, Bertero E, Wilhelm D, Wagner M, Sequeira V, et al. CaMKII does not control mitochondrial Ca²⁺ uptake in cardiac myocytes. *J Physiol.* 2020;598:1361-76. DOI: [10.1113/JP276766](https://doi.org/10.1113/JP276766), PMID: [30770570](https://pubmed.ncbi.nlm.nih.gov/30770570/)